Technical Innovations & Patient Support in Radiation Oncology 6 (2018) 11–19

Contents lists available at ScienceDirect

Technical Innovations & Patient Support in Radiation Oncology

journal homepage: www.elsevier.com/locate/tipsro

Research article

Intensity-modulated radiotherapy for whole pelvis irradiation in prostate cancer: A dosimetric and plan robustness study between photons and protons

Ashley L.K. Ong [a,*], K.W. Ang [a], Zubin Master [a], Sharon M.M. Wong [a,c,d], Jeffrey K.L. Tuan [a,b]

[a] Division of Radiation Oncology, National Cancer Centre Singapore, Singapore
[b] Duke-National University of Singapore Graduate Medical School, Singapore
[c] Health and Social Sciences Cluster, Singapore Institute of Technology, Singapore
[d] College of Allied Health, SingHealth Academy, Singapore

ARTICLE INFO

Article history:
Received 13 December 2017
Received in revised form 16 February 2018
Accepted 22 February 2018
Available online 3 April 2018

Keywords:
Prostate cancer
Pelvic lymph nodes
VMAT
IMPT
PBS
Robust analysis

ABSTRACT

Purpose: To evaluate the dosimetric impact and plan robustness of using Pencil Beam Scanning (PBS) in patients that requires prophylactic pelvic lymph nodes (PLNs) irradiation for prostate cancer.
Material and methods: Five intermediate to high-risk prostate patients previously treated using volumetric modulated arc therapy (VMAT), were selected for this study. Comparative proton radiotherapy plans were generated, where a three-field intensity modulated proton therapy (IMPT) plan was for the phase 1 planning target volume (PTV1) with PLNs. A technique with two posterior oblique fields using single field uniform dose (SFUD) was used for phase 2 (PTV2) volume, that comprises of the prostate and proximal seminal vesicles (Pro + proxSVs). Plan evaluation was performed on PTV coverage and dose to the organs at risk (OARs) using VMAT plans as a baseline (BL). Robust analysis on clinical target volume (CTV) coverage for the PBS plans was simulated with a 3 and 5 mm setup errors and a 3.5% range uncertainty.
Results: For target coverage, PTV1 and PTV2 showed negligible differences with a comparable homogeneity index (HI) values for both modalities. Proton plans produced a statistically significant lower mean dose to the bladder (32.5 Gy(RBE) vs. 46.5 Gy) and rectum (33.6 Gy(RBE) vs. 42.7 Gy). Dose to the bladder and rectum was equivalent at the high dose region. For the bowel cavity, the mean dose for proton plans were 45% lower compared to VMAT plans. Similarly, proton plans were able to achieve an overall reduction in integral dose for both treatment phase. CTV coverage remained high with all the simulated setup and range errors.
Conclusions: Proposed beam geometries for PTV1 and PTV2 proton plans presented good treatment accuracy with similar target coverage as the VMAT plans. Better sparing of OARs was achieved at the low-medium dose region for the proton plans.

Introduction

The use of external beam radiation therapy (EBRT) is a common treatment approach in the management of intermediate to high-risk prostate cancer [1,2]. Routinely, a volumetric modulated arc therapy (VMAT) technique is used for prostate with prophylactic pelvic lymph nodes (PLNs) irradiation, as it is able to achieve superior target coverage with good organs at risk (OARs) sparing. Early clinical studies reported an acceptable rates of acute grade 2 gastrointestinal (GI) and genitourinary (GU) toxicities with VMAT technique [2,3].

As technology advances in the field of proton beam therapy (PBT), there has been a paradigm shifts from the passive scatter technique to an active or pencil beam scanning (PBS) technique, which allows a steeper dose gradient to be achieved with very little dose to the distal region of the target [4]. There are further subdivisions in the PBS techniques, namely single field uniform dose (SFUD) or intensity modulated proton therapy (IMPT).

In SFUD, all spots are optimized independently such that each proton beam provides a homogeneous target coverage [5]. Parallel-opposed SFUD technique is commonly used in prostate alone planning whereby it is able to decrease low-medium dose

* Corresponding author at: Division of Radiation Oncology, National Cancer Centre Singapore, 11 Hospital Drive, Singapore.
E-mail address: ashley.ong.l.k@nccs.com.sg (A.L.K. Ong).

https://doi.org/10.1016/j.tipsro.2018.02.001
2405-6324/

to the bladder and rectum, with significant reduction in low dose bath to the surrounding healthy tissues when compared with VMAT as demonstrated in several studies [6,7]. Although SFUD is less sensitive to setup errors and beam range uncertainty, this optimization method is not suitable in geometrically challenging targets such as whole pelvic radiotherapy (WPRT). The dose distribution is less conformal to the target, with edges of high dose within normal healthy tissues [8]. Sparing of proximal OARs such as the bowels, bladder and rectum is inferior compared to using VMAT.

In IMPT, spots from all proton beams are optimized simultaneously in such a way that each field individually delivers an inhomogeneous dose but when the dose from all fields is summed up, the plan delivers a homogeneous dose across the target volume. This allows us to deliver plans with superior target coverage and/or OARs sparing due to additional modulation possible within the target, like what we achieve in photon-based inverse planning techniques [9]. On the downside, the steep dose gradients within the target increases the susceptibility of IMPT to setup and range errors [10]. There is a great potential of using IMPT to treat concave targets such as WPRT for prostate cancer if a planning method can be devised to overcome the disadvantage of being highly sensitive to uncertainties.

Split target technique using IMPT has been used to treat small complex targets to the thoracic region [11]. The application of this method in large complex volume using the proposed beam geometry in WPRT has not been widely studied. The aim of this pilot study is to propose a technique using IMPT in phase 1 planning that involves a complicated target and SFUD for phase 2 planning in view of the target simplicity. A dosimetric comparison in terms of target coverage and dose to OARs will be carried out using plans generated with VMAT as baseline (BL). Plan robustness test of the proposed beam geometry in the event of patient setup error and range uncertainty will be analyzed for clinical target volume (CTV) coverage.

Material and methods

Institutional review committee approval was obtained for this retrospective dosimetric study. This pilot study included five intermediate to high-risk prostate patients with PLNs irradiation.

Simulation

All prostate cancer patients underwent a computed tomography (CT) simulation on a GE Lightspeed RT16 CT scanner (GE Healthcare, Chicago, Illinois, US) in a supine position with arms on the chest, using a0.25 slice thickness. A leg immobiliser was used for stabilisation and reproducibility. As per institutional protocol, a comfortably full bladder was achieved by requesting patients to first empty their bladder and then drink 2 cups of water (400 ml) 30 min prior to the CT simulation scan. The same protocol was continued for each radiotherapy treatment session. No specific rectal preparation protocol was enforced, but all patients were encouraged to empty their bowels prior to the CT simulation scan and before each treatment fraction. The CT datasets were transferred to the treatment planning system (TPS) for contouring and planning.

Target definition and dose prescription

Five intermediate to high-risk Prostate cancer patients previously treated with VMAT were selected for proton planning. For each patient, two proton plans were generated; planning target volume (PTV) 1 and PTV 2 respectively. This is a sequential treatment with the following target volume definitions and prescriptions:

PTV 1 was generated with a 0.5–0.7 cm expansion from PLNs CTV, 1 cm margin around prostate and seminal vesicles (Pro + SVs) except posteriorly, a 0.6 cm margin was given. 45 Gy in 25 fractions with 1.8 Gy per fraction was prescribed; PTV 2 was generated with a 1 cm expansion from CTV 2 (prostate and proximal seminal vesicles; Pro + proxSVs) and a 0.6 cm posterior margin. 34.2 Gy in 19 fractions with 1.8 Gy per fraction was prescribed. All OARs such as the rectum, bladder, bowel cavity and femurs were contoured as per RTOG contouring guidelines. Table 1 indicates the dose volume constraints for target coverage and OARs.

Treatment planning

Treatment planning for both modalities was performed using Eclipse treatment planning system (TPS) version 13.6 (Varian Medical Systems, Palo Alto, CA, US). All calculated plans were normalized such that at least 95% of the PTV volume received the prescription dose.

VMAT planning

VMAT plan for PTV 1 consists of two full arcs (179–181°; clockwise, 181–179°; counter clockwise) with a collimator tilt of 30°/330°. For PTV 2, an arc angle of 200–160° clockwise and 200–160° counter clockwise with a collimator tilt of 15°/345° was used. Plans were generated with a 10 MV energy and at a maximum dose rate (DR) of 600 MU/min. VMAT plans were optimized using the Photon Optimizer (PO) to achieve the desired dose volume constraints by continuously varying the DR, multileaf collimator (MLC) positions and gantry rotational speed to optimize the dose distribution. Details about VMAT optimization process has been published elsewhere [12]. Planning optimization objectives were adjusted to prioritize target coverage while minimizing the dose to the OARs, especially at the high dose region of the rectum. Final dose calculations were done using anisotropic analytical algorithm (AAA) with a dose calculation grid size of 2.5 mm.

Table 1
Dose-volume constraints for target volumes and OARs.

Structures	Objectives
PTV1 and PTV2	$D_{95\%} \geq$ PD $D_{2\%} <$ 107%
CTV1 and CTV2	$D_{98\%} \geq$ PD $D_{2\%} <$ 107%
Rectum	$V_{50Gy} <$ 60% $V_{35Gy} <$ 65% $V_{25Gy} <$ 70% $V_{15Gy} <$ 75%
Bladder	$V_{50Gy} <$ 65% $V_{35Gy} <$ 70% $V_{25Gy} <$ 75% $V_{15Gy} <$ 80%
Bowel cavity	$V_{30Gy} <$ 40%
Femurs	$V_{5Gy} <$ 50%

PTV, planning target volume; CTV, clinical target volume; OARs, organs at risk; PD, prescription dose; Dx, dose received by target at a defined volume (x) in percentage; Vx, volume of OAR receiving a defined dose (x) in Gray.

Proton planning

In terms of beam geometry, PBS plan for PTV 1 comprises of a three-field method whereby each individual field (right and left lateral) covers each side of the PLNs. Both fields included the prostate (inferiorly) and the distal common iliac vessels (superiorly). The third field is a single posterior beam that encompassed the whole PTV (Fig. 1). IMPT technique was used for plan optimization for PTV 1 in view of target complexity, whilst for PTV 2, two equally weighted posterior oblique beams using SFUD technique was used.

A non-clinical proton beam data with an energy range of 68–250 MeV and an approximate spot spacing at isocenter of 0.65 times the full width at half-maximum (FWHM) of the spot in air was used for each field. A Nonlinear Proton Optimizer (NUPO) was used for optimization with a similar set of optimization objectives as in VMAT planning. Final dose calculation was done using Proton.

Convolution Superposition algorithm whereby the absorbed dose was expressed in Gray-Equivalent (Gy(RBE)) for protons with a constant Relative Biological Effective dose (RBE) of 1.1. For dosimetric comparative purpose, proton planning was performed using the same PTV definition as VMAT. Table 2 indicates the proton planning parameters used in PTV 1 and PTV 2.

Plan evaluation tools

Dosimetric metrics used for evaluating target coverage and OARs dose were extracted from the dose-volume histograms (DVHs). This includes:

- Dx; dose received by a structure at a defined volume (x) in percentage,
- Vx, volume of the structure receiving a defined dose (x) in Gray,
- D_{mean}; mean dose received by a structure,
- Homogeneity Index (HI); measurement of dose uniformity within the target [13].

$$HI = \frac{D2\% - D98\%}{D50\%}$$

- Conformation Number (CN); measurement of the degree of high dose conformation to the target [14].

$$CN = \frac{TVRI}{TV} + \frac{TVRI}{VRI}$$

- Whereby TVRI: Target covered by reference isodose,
- TV: Target Volume,
- VRI: Volume of reference isodose,
- Integral Dose (ID) received by the patient is defined as the mean dose deposited in the body multiply by the body volume being irradiated [13].

Table 2
PBS planning parameters for PTV 1 and PTV 2.

Parameters	PTV 1	PTV 2
PBS technique	IMPT	SFUD
Nominal energy (MeV)	190.83 ± 16.02 (163.93–206.61)	184.19 ± 5.87 (174.68 ± 189.64)
No. of layers	27 ± 3 (22–31)	11 ± 1 (10–13)
Spot spacing (mm)	5	5
Gantry angles	G: 270°, 90°, 180°	G: 260°, 100°
Target margin (mm)		
Proximal	2	2
Distal	7	5
Lateral	7	7

PTV, planning target volume; PBS, pencil beam scanning; IMPT, intensity modulated proton therapy; SFUD, single-field uniform dose; MeV, megavoltage; G, gantry.

Table 3
Average BL CTV values for five non-perturbed cases.

CTV	Parameters
CTV1_PLNs	
$D_{98\%}$ (Gy(RBE))	45.42 ± 0.10
$V_{45Gy(RBE)}$ (%)	99.82 ± 0.18
$D_{2\%}$ (Gy(RBE))	46.64 ± 0.17
$HI_{2-98\%}$	0.03 ± 0.00
CTV1_Pro+SVs	
$D_{98\%}$ (Gy(RBE))	45.40 ± 0.13
$V_{45Gy(RBE)}$ (%)	99.99 ± 0.03
$D_{2\%}$ (Gy(RBE))	46.44 ± 0.17
$HI_{2-98\%}$	0.02 ± 0.00
CTV2_Pro+proxSVs	
$D_{98\%}$ (Gy(RBE))	34.45 ± 0.14
$V_{45Gy(RBE)}$ (%)	99.87 ± 0.25
$D_{2\%}$ (Gy(RBE))	35.21 ± 0.24
$HI_{2-98\%}$	0.02 ± 0.01

CTV, clinical target volume; Gy(RBE); gray(radiobiological equivalent); Dx, dose received by target at a defined volume (x) in percentage; Vx, volume of target receiving a defined dose (x) in Gray; HI, homogeneity index; PLNs, pelvic lymph nodes; Pro + SVs, prostate and seminal vesicles; Pro + proxSVs, prostate and proximal seminal vesicles; $^{*}p < 0.05$, statistically significant.

$$ID\ (Gy \cdot L) = \text{Bodymean(Gy)} \times \textit{Body Volume}\ (\textit{Litres})$$

Plan robustness analysis

Plan robustness analysis was performed using the plan uncertainty evaluation tool in Eclipse TPS. Both translation (anterior-posterior; A-P, superior-inferior; S-I, left-right; L-R) and range errors (Hounsfield unit (HU): ±3.5%) were simulated separately,

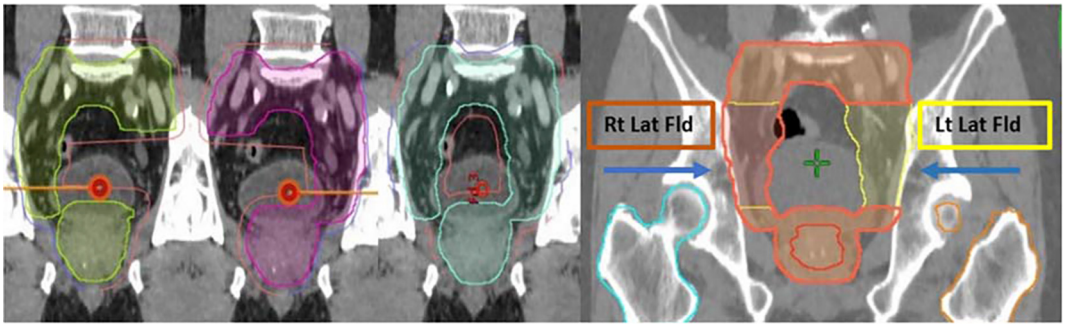

Fig. 1. Coronal view on target margin expansion (left) and beam geometry (right) for PTV1 of a pencil bean scanning (PBS) plan.

resulting in a total of 14 dose perturbations for each proton plan. For CTV1, PLNs and Pro + SVs were assessed independently whilst for CTV2, Pro + proxSVs was measured. BL CTV1 and CTV2 values were recorded for the non-perturbed plans for comparison (Table 3).

Robustness analysis was not conducted in VMAT plans in view of the "static dose cloud approximation" theory whereby minor changes in setup error will have a negligible impact in dose distribution with the use of a PTV concept in photon treatment [15].

Data and statistical analysis

The paired, two tails Student's t-test was used for comparison of results between photon and PBS plans. The data were performed

Table 4
Dosimetric comparisons for target coverage between VMAT and PBS.

Target	Parameter	VMAT	PBS (Gy(RBE))	P-value
PTV1	$D_{95\%}$ (Gy)	45.07 ± 0.10	45.36 ± 0.24	0.027*
	$D_{2\%}$ (Gy)	46.93 ± 0.14	46.86 ± 0.15	0.361
	Dmean (Gy)	45.94 ± 0.12	46.05 ± 0.05	0.128
	$V_{105\%}$ (cm3)	2.34 ± 2.96	1.44 ± 1.39	0.601
	$CN_{95\%}$	0.76 ± 0.02	0.77 ± 0.89	0.856
	$CN_{100\%}$	0.89 ± 0.03	0.96 ± 0.04	0.843
	$HI_{2\text{-}98\%}$	0.05 ± 0.01	0.04 ± 0.01	0.587
Vol. cm^3	729.29 ± 131.77 (576.25–893.97)			
PTV2	$D_{95\%}$ (Gy)	34.33 ± 0.11	34.39 ± 0.08	0.227
	$D_{2\%}$ (Gy)	35.45 ± 0.34	35.52 ± 0.17	0.670
	D_{mean} (Gy)	34.89 ± 0.24	34.87 ± 0.03	0.902
	$V_{105\%}$ (cm^3)	0.29 ± 0.47	0.25 ± 0.44	0.570
	$CN_{95\%}$	0.78 ± 0.04	0.78 ± 0.93	0.905
	$CN_{100\%}$	0.92 ± 0.05	0.03 ± 0.04	0.827
	$HI_{2\text{-}98\%}$	0.04 ± 0.01	0.04 ± 0.01	0.749
Vol. cm^3	89.64 ± 16.80 (69.23–109.21)			

PTV, planning target volume; Gy(RBE); gray(radiobiological equivalent); VMAT, volumetric modulated arc therapy; PBS, pencil beam scanning; Dx, dose received by target at a defined volume (x) in percentage; Vx, volume of target receiving a defined dose (x) in Gray; CN, conformation number; HI, homogeneity index; *p < 0.05, statistically significant.

Table 5
Dosimetric comparisons for OARs between VMAT and PBS.

Organ	Parameter	VMAT	PBS (Gy(RBE))	P-value
Rectum	V_{30Gy} (%)	69.90 ± 5.69	46.89 ± 14.68	0.010*
	V_{40Gy} (%)	49.78 ± 11.50	34.52 ± 13.86	0.001*
	V_{50Gy} (%)	34.74 ± 11.35	24.60 ± 11.40	0.007*
	V_{60Gy} (%)	22.22 ± 8.94	17.80 ± 9.39	0.034*
	V_{70Gy} (%)	12.11 ± 6.41	11.82 ± 7.08	0.657
	V_{75Gy} (%)	7.83 ± 4.94	8.60 ± 5.56	0.135
	$D_{1\%}$ (Gy)	79.21 ± 2.45	78.28 ± 4.46	0.408
	D_{mean} (Gy)	42.68 ± 4.60	33.60 ± 7.64	0.003*
Vol. overlap with PTV1 (cm^3): 3.57 ± 2.28 (0.01–6.17)				
Vol. overlap with PTV2 (cm^3): 1.58 ± 1.27 (0.01–3.09)				
Bladder	V_{35Gy} (%)	72.89 ± 6.24	44.99 ± 2.27	0.000*
	V_{40Gy} (%)	54.62 ± 1.89	40.11 ± 1.72	0.000*
	V_{50Gy} (%)	30.57 ± 5.13	26.26 ± 2.84	0.018*
	V_{60Gy} (%)	20.95 ± 2.82	20.04 ± 2.45	0.111
	V_{70Gy} (%)	14.21 ± 1.36	14.73 ± 1.76	0.207
	V_{75Gy} (%)	11.43 ± 1.30	11.69 ± 1.29	0.34
	$D_{1\%}$ (Gy)	81.55 ± 0.48	81.67 ± 0.24	0.488
	D_{mean} (Gy)	46.51 ± 0.89	32.47 ± 1.03	0.000*
Vol. overlap with PTV1 (cm^3): 32.12 ± 12.36 (20.61–48.69)				
Vol. overlap with PTV2 (cm^3): 12.19 ± 2.21 (9.24–14.62)				
Bowel cavity	V_{20Gy} (%)	50.62 ± 11.53	24.80 ± 4.78	0.004*
	V_{30Gy} (%)	30.19 ± 5.68	20.26 ± 3.86	0.003*
	V_{45Gy} (cm^3)	201.19 ± 80.81	198.10 ± 91.30	0.321
	$D_{1\%}$ (Gy)	47.48 ± 0.86	46.77 ± 0.16	0.082
	D_{mean} (Gy)	21.11 ± 3.25	11.56 ± 2.26	0.000*
Vol. overlap with PTV1 (cm^3): 182.74 ± 66.50 (92.58–273.07)				
Rt Femur	$D_{50\%}$ (Gy)	19.26 ± 1.19	19.70 ± 3.24	0.776
	$D_{1\%}$ (Gy)	43.50 ± 2.49	29.84 ± 3.80	0.002*
	D_{mean} (Gy)	19.85 ± 1.07	17.86 ± 1.77	0.036*
Lt Femur	$D_{50\%}$ (Gy)	18.67 ± 1.22	19.56 ± 3.62	0.49
	$D_{1\%}$ (Gy)	42.46 ± 4.50	31.21 ± 3.42	0.003*
	D_{mean} (Gy)	19.38 ± 1.80	17.69 ± 2.35	0.007*
ID (Gy.L)	ID PTV1	222.68 ± 20.96	123.58 ± 10.36	0.000*
	ID PTV2	37.96 ± 4.88	18.75 ± 4.99	0.000*

Gy(RBE); gray(radiobiological equivalent); VMAT, volumetric modulated arc therapy; PBS, pencil beam scanning; ID, integral dose; Dx, dose received by an organ at risk at a defined volume (x) in percentage; Vx, volume of the organ at risk receiving a defined dose (x) in Gray; *p < 0.05, statistically significant.

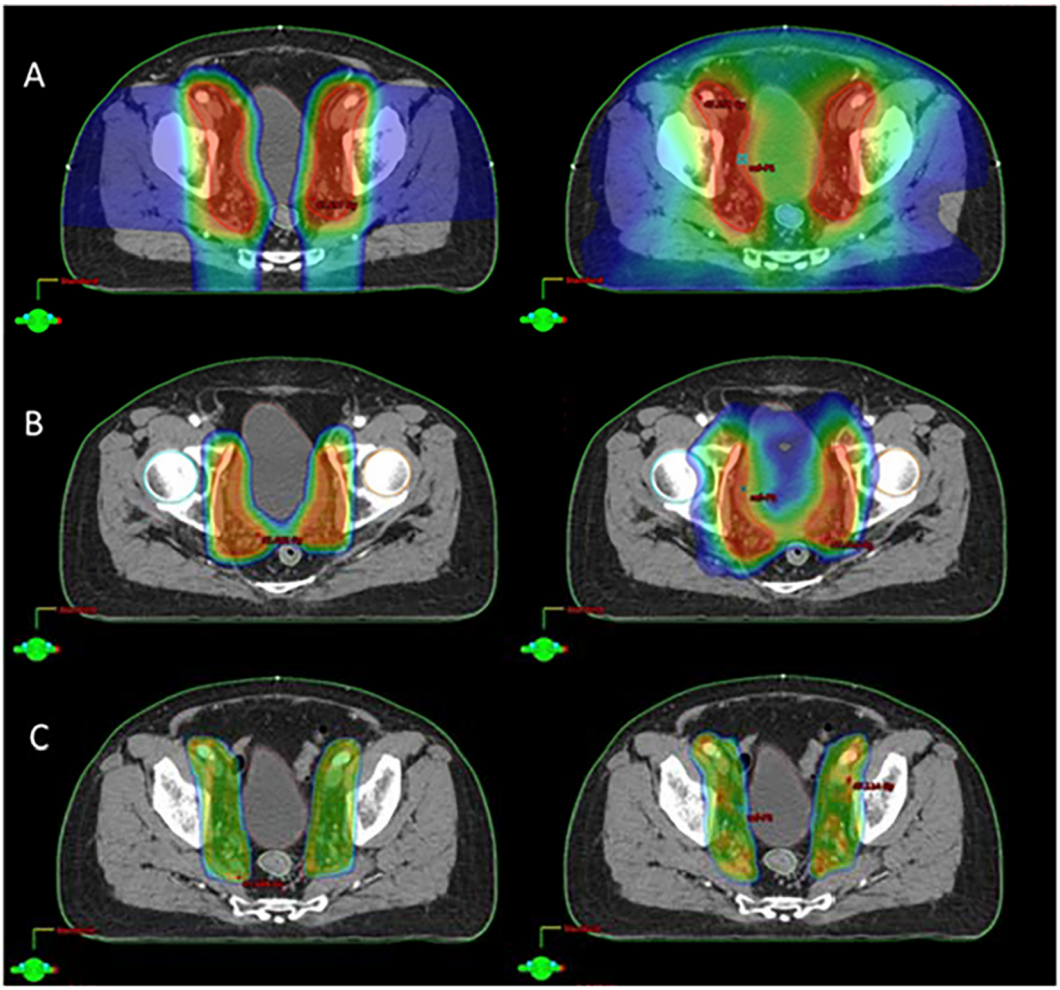

Fig. 2. Dose distribution for PTV 1 IMPT (Lt) and VMAT (Rt) plans for one patient; (A) colourwash at 10 Gy, (B) 30 Gy, (C) 42.75 Gy. (For interpretation of the references to colour in this figure legend, the reader is referred to the web version of this article.)

using SPSS version 24.0.0 (Armonk, NY: IBM Corp) with $p < 0.05$ was considered significant.

Results

Dosimetric comparisons for target coverage and OARs dose between VMAT and PBS are shown in Tables 4 and 5 respectively.

Target volume

For target dose, PTV1 and PTV2 showed good coverage whereby D95% of the target received the prescribed dose (PTV1_ 45.36 ± 0.24 Gy(RBE) vs. 45.07 ± 0.10 Gy; PTV2_ 34.39 ± 0.08 Gy(RBE) vs. 34.33 ± 0.11 Gy) and having a similar HI values for both modalities. Likewise, dose conformity for PTV1 and PTV 2 are comparable. Dose distribution for PTV 1 and PTV 2 are represented in Figs. 2 and 3 respectively.

OARs

Proton plans produced a statistically significant lower mean dose to the bladder (32.47 ± 1.03 Gy(RBE) vs. 46.51 ± 0.89 Gy) and rectum (33.60 ± 7.64 Gy(RBE) vs. 42.68 ± 4.60 Gy) at the low to intermediate dose region (V30Gy to V50Gy). Whilst at high dose region, dose to the bladder and rectum were comparable. For the bowel cavity, the mean dose for proton plans were approximately 45% lower compared to VMAT plans. For the femurs, dose to D50% were equivalent for both modalities but dose at D1% were very much reduced and were significant in the proton plans with 68.6% (Rt) and 73.5% (Lt) difference.

Integral dose

In terms of integral dose, PTV 1 PBS plans result in a 55.5% lower dose to the healthy tissues whilst for PTV 2 PBS plans, a decrease of 49.4% was achieved. PBS plans result in a statistically significant overall decreased in integral dose.

Robustness analysis

Tables 6–8 demonstrated the effects of setup and range errors on CTVs for CTV1_PLNs, CTV1_ProSVs and CTV2_Pro+proxSVs respectively.

CTV1_PLNs

For CTV1_PLNs plans, all simulated dose perturbations achieved a D98% CTV coverage of 45 Gy(RBE) apart from a range error of −3.5%, whereby the mean difference is 2% lesser than BL plans. There was a statistically significant increase in D2% for 5 mm setup error shifts, indicating an overall increased in hotspots within the

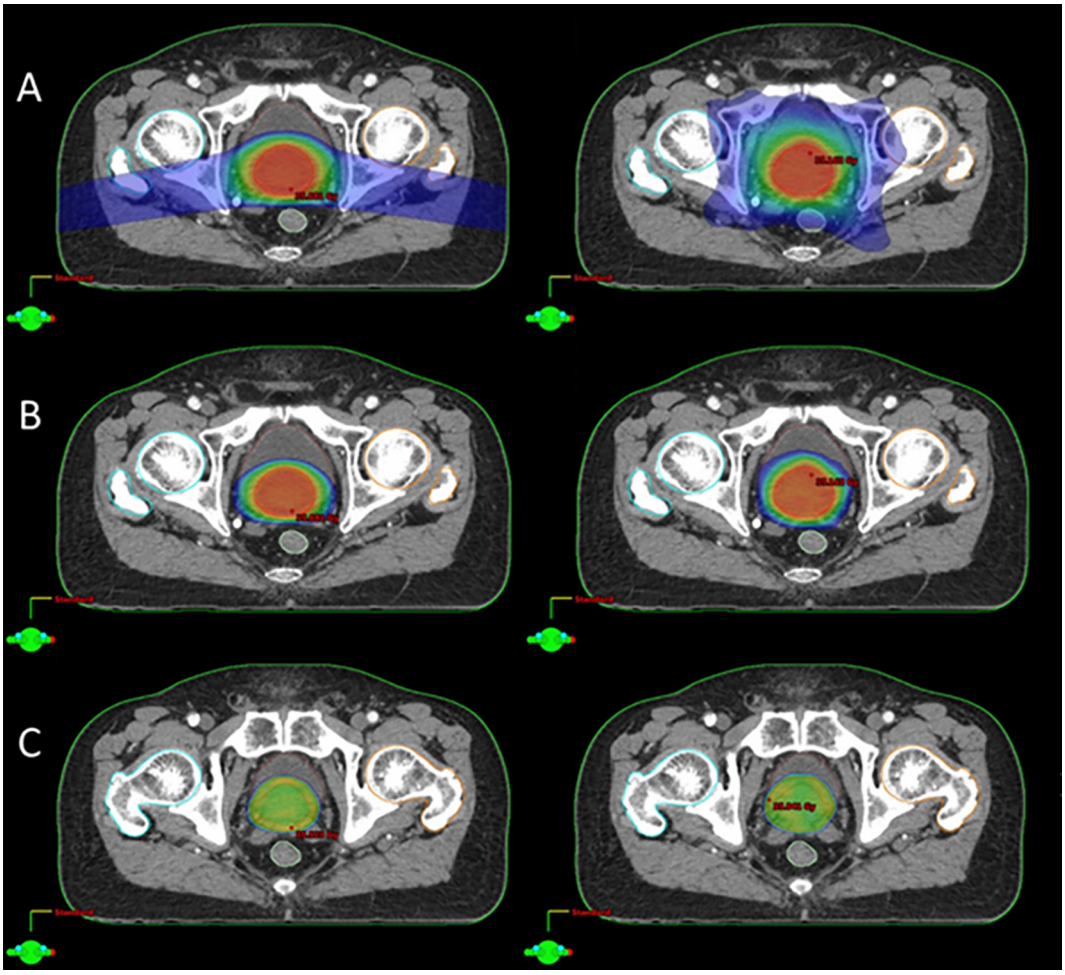

Fig. 3. Dose distribution for PTV 2 SFUD (Lt) and VMAT (Rt) plans for one patient; (A) colourwash at 10Gy, (B) 20Gy, (C) 32.5Gy. (For interpretation of the references to colour in this figure legend, the reader is referred to the web version of this article.)

target. HI of the plans was also affected by a setup error of 5 mm in all directions, except for an error in the superior direction.

CTV1_Pro+SVs

For CTV1_Pro+SVs plans, V45Gy(RBE) CTV coverage in the Lt-Rt setup error direction (+3 mm: 99.78, −3 mm: 99.79, +5 mm: 98.80 vs BL: 99.99) indicates a statistical significant difference from BL plans. Likewise, Lt-Rt setup errors also resulted in a difference in HI values at ±5 mm (+5 mm: 0.04, −5 mm: 0.04 vs BL: 0.02).

CTV2_Pro+proxSVs

In CTV2_Pro+proxSVs plans, although there is a statistical significant difference for D98% coverage in the +5 mm direction and at a range uncertainty of +3.5%, the average dose to D98% of CTVs is still above the prescribed dose. There is an overall negligible difference in terms of target coverage and hotspots within the volume.

Discussion

The role of prophylactic PLNs irradiation is debatable, ongoing RTOG 0924 trial (NCT01368588) should shed more light on the patient outcomes after trial completion [16,17]. In this study, the recommended beam geometry and split-field method for PTV 1 using IMPT is able to achieve a comparable target coverage as the VMAT plans. In plan summation with the proposed posterior oblique fields for PTV 2 using SFUD, there is a substantial dose reduction in the low to intermediate dose range for all the OARs. Similar observations were noted in a study conducted by Widesott et al., whereby dosimetric comparisons were made in high-risk prostate cancer patients involving PLNs using helical Tomotherapy (HT) and IMPT plans [18].

Dose reduction at the low to intermediate dose range using PBS is critical in minimizing acute toxicity. A recent publication from the proton collaborative group REG001-09 trial concluded that less acute GI toxicity was reported with IMPT treatment for prostate with PLNs [19]. A strong correlation exists between a low small bowel dose and associated acute GI toxicity as established by studies using proton treatment to the pelvis [20,21]. In terms of acute GU toxicity, it was reported that there is no difference between PBT and intensity modulated radiotherapy (IMRT) technique, as dose to the urethra might be the reason for the observation. An association with the prescribed prostate dose with either acute or late GU toxicity might exist [22,23].

The volume of rectum receiving 70 Gy or more is similar in both PBS and VMAT plans. This result is expected in view of the close proximity of the rectum to the high dose region. In terms of integral dose received by the patient, PBS plans result in a dramatic reduction of dose to the healthy tissues. This significant decreased in low dose exposure to the rest of the body is crucial in reducing the calculated risk of secondary malignancies [24].

In plan robustness analysis, a simulated random setup error of 3 and 5 mm and a systematic range error of 3.5% were performed.

Table 6
Effect of setup and range errors on CTV1_PLNs in phase 1 PBS plans.

Setup/range errors		CTV1_PLNs			
		$D_{98\%}$ (Gy(RBE))	$V_{45Gy(RBE)}$ (%)	$D_{2\%}$ (Gy(RBE))	$HI_{2-98\%}$
Setup: A-P	+3 mm	45.22 ± 0.14*	99.25 ± 0.61	46.63 ± 0.14	0.03 ± 0.00
y	+5 mm	45.00 ± 0.18*	97.96 ± 1.12*	46.59 ± 0.10	0.04 ± 0.00*
	−3 mm	45.39 ± 0.13	99.51 ± 0.56	46.74 ± 0.23	0.03 ± 0.00
	−5 mm	45.31 ± 0.19	99.20 ± 0.87	46.99 ± 0.13*	0.04 ± 0.00*
Setup: S-I	+3 mm	45.42 ± 0.06	99.82 ± 0.17	46.76 ± 0.14	0.03 ± 0.00
z	+5 mm	45.37 ± 0.09	99.63 ± 0.33	46.93 ± 0.15*	0.03 ± 0.00*
	−3 mm	45.39 ± 0.13	99.75 ± 0.36	46.71 ± 0.18	0.03 ± 0.01
	−5 mm	45.23 ± 0.20	98.87 ± 0.77	46.79 ± 0.14	0.03 ± 0.01
Setup: L-R	+3 mm	45.38 ± 0.10	99.72 ± 0.26	46.84 ± 0.17	0.03 ± 0.01
x	+5 mm	45.31 ± 0.11	99.32 ± 0.29*	47.24 ± 0.48	0.04 ± 0.01
	−3 mm	45.31 ± 0.19	99.36 ± 0.85	46.80 ± 0.13	0.03 ± 0.01
	−5 mm	45.18 ± 0.24	98.80 ± 0.91	47.06 ± 0.20*	0.04 ± 0.01*
Range (HU)	+3.5%	44.54 ± 1.2	97.43 ± 2.82	47.04 ± 0.27*	0.07 ± 0.03
	−3.5%	45.23 ± 0.08*	99.48 ± 0.38	47.22 ± 0.56	0.04 ± 0.01*

CTV, clinical target volume; Gy(RBE); gray(radiobiological equivalent); PLNs, pelvic lymph nodes; Dx, dose received by the target at a defined volume (x) in percentage; Vx, volume of the target receiving a defined dose (x) in Gray; HI, homogeneity index; HU, hounsfield units; A-P, anterior-posterior; S-I, superior-inferior; L-R, left-right; *$p < 0.05$, statistically significant.

Table 7
Effect of setup and range error on CTV1_Pro+SVs in phase 1 PBS plans.

Setup/range errors		CTV1_Pro+SVs			
		$D_{98\%}$ (Gy(RBE))	$V_{45Gy(RBE)}$ (%)	$D_{2\%}$ (Gy(RBE))	$HI_{2-98\%}$
Setup: A-P	+3 mm	45.40 ± 0.07	100.00 ± 0.00	46.44 ± 0.22	0.02 ± 0.00
y	+5 mm	45.29 ± 0.09	99.86 ± 1.17	46.57 ± 0.27	0.03 ± 0.00
	−3 mm	45.35 ± 0.19	99.65 ± 0.59	46.57 ± 0.11	0.03 ± 0.01
	−5 mm	45.27 ± 0.31	99.17 ± 1.56	46.68 ± 0.14*	0.03 ± 0.01
Setup: S-I	+3 mm	45.33 ± 0.16	99.85 ± 0.19	46.48 ± 0.14	0.03 ± 0.00
z	+5 mm	45.24 ± 0.19	99.42 ± 0.68	46.53 ± 0.31	0.03 ± 0.01
	−3 mm	45.41 ± 0.10	99.94 ± 0.08	46.47 ± 0.15	0.02 ± 0.01
	−5 mm	45.30 ± 0.21	99.39 ± 0.93	46.56 ± 0.11	0.03 ± 0.01
Setup: L-R	+3 mm	45.29 ± 0.08	99.78 ± 0.16*	46.63 ± 0.25	0.03 ± 0.00
x	+5 mm	45.12 ± 0.11*	98.80 ± 0.82*	46.82 ± 0.42	0.04 ± 0.01*
	−3 mm	45.33 ± 0.06	99.79 ± 0.16*	46.42 ± 0.24	0.03 ± 0.00
	−5 mm	45.19 ± 0.14*	99.12 ± 0.75	46.81 ± 0.35	0.04 ± 0.01*
Range (HU)	+3.5%	45.52 ± 0.13	99.93 ± 0.11	46.64 ± 0.11	0.02 ± 0.01
	−3.5%	45.06 ± 0.12*	98.63 ± 1.33	46.41 ± 0.27	0.03 ± 0.01

CTV, clinical target volume; Gy(RBE); gray(radiobiological equivalent); Pro + SVs, prostate and seminal vesicles; Dx, dose received by the target at a defined volume (x) in percentage; Vx, volume of the target receiving x dose in Gray; HI, homogeneity index; HU, hounsfield units; A-P, anterior-posterior; S-I, superior-inferior; L-R, left-right; *$p < 0.05$, statistically significant.

Dose perturbation as a result of a 5 mm misalignments were more significant in CTV1_PLNs plans compared to the BL plans. However, the impact to CTV1_PLNs coverage was minimal as D98% of the target still received the prescribed dose. As demonstrated in studies using SFUD method for plan optimization, CTV2_Pro+proxSVs plans remain relatively robust, whereby the CTV coverage remained high [7,25].

The simulated errors can be considered as an over-estimation as these errors are unlikely to happen in every treatment fraction [26]. Rotational errors were not simulated in this study as it has been reported that with a rotational misalignment of ±3/5 mm, CTV coverage as well as dose to the bladder and rectum were modestly affected [27].

From the tabulated results, it has been observed that dose variation in the CTV happens more frequently in simulated range errors than in setup errors. Similar sensitivity of CTV to range errors were also reported by Safai et al. whereby plan comparisons were made in geometrically challenging cases using 3 dimensional conformal proton therapy (3DCPT) and IMPT [9]. Accurate estimation of range error is a challenge in proton therapy planning. Typically, a 3–3.5% with additional 1–3 mm range margin is often used by centres to estimate the CT calibration curve to proton stopping power error [28].

However, recent studies conducted on the potential use of dual-energy CT (DECT) in proton therapy found that it is able to provide a better proton beam range predictions with an estimated error of approximately 1–2% [29,30]. These findings have the potential to improve clinical outcomes by reducing the safety margins used in proton planning, thus limiting unnecessary exposure of healthy tissues to high dose radiation [30].

There are a few limitations in this study. Inter and intrafractional potential variables that will cause density alterations along the beam path such as the presence of rectal and bowel gas were not accounted for in this study. Although it has been demonstrated that with the absent of water equivalent density override of rectal cavities will result in an inferior target coverage, the cases presented have minimal rectal gas observed as patients were encouraged to empty their bowel [31].

Moreover, a strict simulation guideline in terms of limiting maximum rectal dimension (due to the presence of gas cavities or faecal content) is routinely conducted for all prostate cases.

Table 8
Effect of setup and range uncertainties on CTV2_Pro+proxSVs in phase 2 PBS plans.

Setup/range errors		CTV2_Pro+proxSVs			
		$D_{98\%}$ (Gy(RBE))	$V_{45Gy(RBE)}$ (%)	$D_{2\%}$ (Gy(RBE))	$HI_{2-98\%}$
Setup: A-P	+3 mm	34.35 ± 0.13	99.39 ± 1.06	35.25 ± 0.23	0.02 ± 0.01
y	+5 mm	34.21 ± 0.13*	97.49 ± 3.12	35.34 ± 0.22	0.02 ± 0.01
	−3 mm	34.39 ± 0.12	99.49 ± 0.82	35.33 ± 0.20	0.02 ± 0.01
	−5 mm	34.31 ± 0.13	98.93 ± 1.25	35.47 ± 0.14	0.03 ± 0.01
Setup: S-I	+3 mm	34.41 ± 0.12	99.78 ± 0.36	35.23 ± 0.20	0.02 ± 0.01
z	+5 mm	34.33 ± 0.11	99.21 ± 0.83	35.35 ± 0.16	0.02 ± 0.01
	−3 mm	34.41 ± 0.14	99.65 ± 0.66	35.29 ± 0.25	0.02 ± 0.01
	−5 mm	34.33 ± 0.15	99.02 ± 1.36	35.38 ± 0.28	0.02 ± 0.01
Setup: L-R	+3 mm	34.45 ± 0.14	99.87 ± 0.21	35.21 ± 0.23	0.02 ± 0.01
x	+5 mm	34.44 ± 0.14	99.87 ± 0.18	35.18 ± 0.15	0.02 ± 0.01
	−3 mm	34.45 ± 0.14	99.85 ± 0.30	35.21 ± 0.25	0.02 ± 0.01
	−5 mm	34.45 ± 0.14	99.82 ± 0.33	35.21 ± 0.24	0.02 ± 0.01
Range (HU)	+3.5%	34.71 ± 0.11*	100.00 ± 0.00	35.38 ± 0.18	0.01 ± 0.01
	−3.5%	34.31 ± 0.12	98.54 ± 2.60	35.01 ± 0.21	0.02 ± 0.01

CTV, clinical target volume; Gy(RBE); gray(radiobiological equivalent); Pro + proSVs, prostate and proximal seminal vesicles, Dx, dose received by the target at a defined volume (x) in percentage; Vx, volume of the target receiving x dose in Gray; HI, homogeneity index; HU, hounsfield units; A-P, anterior-posterior; S-I, superior-inferior; L-R, left-right; *$p < 0.05$, statistically significant.

With regards to the uncertainties of intrafractional bowel motion as well as the absent of water equivalent density override for the bowel cavities, this will not posed an issue in this study given that there is no anterior beam entry in the proposed beam geometry. A study conducted by Berger et al. on the effect of bowel gas cavities on proton dose degradation using IMPT concluded that on daily-accumulated dose, this uncertainty has minimal impact on target coverage and dose to OARs [32].

Future study will include exploring the use of robust optimization in proton planning to address the issues of dose sensitivity in IMPT. As the designing of a beam-specific PTV will be able to overcome errors pertaining to SFUD planning, the use of robust optimization will be more relevant in IMPT planning [25]. In view of the presence of highly modulated dose gradients within the target, robust optimization process will take into consideration the various uncertainties (e.g. setup error, tumour motion and range errors) and compensate for perturbations in dose distributions within the targets and OARs to enhance proton plan reliability [33,34].

Conclusions

The proposed beam configurations and split-field technique for treating prostate cancer with PLNs is robust against simulated setup and beam range uncertainties without compromising on PTV coverage. Significant dosimetric gain was observed with PBS plans whereby a reduction of dose in the low to intermediate dose region was achieved for the bladder, small bowel and rectum.

Disclosure statement

The authors of this article report no conflict of interest.

References

[1] Hesselberg G, Fogarty G, Haydu L, Dougheney N, Stricker P. Volumetric modulated arc therapy of the pelvic lymph nodes to the aortic bifurcation in higher risk prostate cancer: early toxicity outcomes. Biomed Res Int 2015;2015:696439.
[2] Ishii K, Ogino R, Hosokawa Y, Fujioka C, Okada W, Nakahara R, et al. Whole-pelvic volumetric-modulated arc therapy for high-risk prostate cancer: treatment planning and acute toxicity. J Radiat Res 2015;56(1):141–50.
[3] Hall WA, Colbert L, Nickleach D, Shelton J, Marcus DM, Switchenko J, et al. Reduced acute toxicity associated with the use of volumetric modulated arc therapy for the treatment of adenocarcinoma of the prostate. Pract Radiat Oncol 2013;3(4):e157–64.
[4] Wayne DN, Rui Z. The physics of proton therapy. Phys Med Biol 2015;60(8):R155.
[5] Mohan R, Das IJ, Ling CC. Empowering intensity modulated proton therapy through physics and technology: an overview. Int J Radiat Oncol Biol Phys 2017;99(2):304–16.
[6] Rana S, Cheng C, Zheng Y, Risalvato D, Cersonsky N, Ramirez E, et al. Proton therapy vs. VMAT for prostate cancer: a treatment planning study. IJPT 2014;1(1):22–33.
[7] Meyer J, Bluett J, Amos R, Levy L, Choi S, Nguyen QN, et al. Spot scanning proton beam therapy for prostate cancer: treatment planning technique and analysis of consequences of rotational and translational alignment errors. Int J Radiat Oncol Biol Phys 2010;78(2):428–34.
[8] Levin WP, Kooy H, Loeffler JS, DeLaney TF. Proton beam therapy. Br J Cancer 2005;93(8):849–54.
[9] Safai S, Trofimov A, Adams JA, Engelsman M, Bortfeld TR. The rationale for intensity modulated proton therapy (IMPT) in geometrically challenging cases. Phys Med Biol 2013;58(18). https://doi.org/10.1088/0031-9155/58/18/633.
[10] Lomax AJ. Intensity modulated proton therapy and its sensitivity to treatment uncertainties 1: the potential effects of calculational uncertainties. Phys Med Biol 2008;53(4):1027–42.
[11] Lomax AJ, Boehringer T, Coray A, Egger E, Goitein G, Grossmann M, et al. Intensity modulated proton therapy: a clinical example. Med Phys 2001;28(3):317–24.
[12] Cozzi L, Dinshaw KA, Shrivastava SK, Mahantshetty U, Engineer R, Deshpande DD, et al. A treatment planning study comparing volumetric arc modulation with RapidArc and fixed field IMRT for cervix uteri radiotherapy. Radiother Oncol 2008;89(2):180–91.
[13] Hodapp N. The ICRU Report 83: prescribing, recording and reporting photon-beam intensity-modulated radiation therapy (IMRT). 2012; 188(1):97–9.
[14] Feuvret L, Noel G, Mazeron JJ, Bey P. Conformity index: a review. Int J Radiat Oncol Biol Phys 2006;64(2):333–42.
[15] Unkelbach J, Bortfeld T, Martin BC, Soukup M. Reducing the sensitivity of IMPT treatment plans to setup errors and range uncertainties via probabilistic treatment planning. Med Phys 2009;36(1):149–63.
[16] Lawton CA, DeSilvio M, Roach 3rd M, Uhl V, Kirsch R, Seider M, et al. An update of the phase III trial comparing whole pelvic to prostate only radiotherapy and neoadjuvant to adjuvant total androgen suppression: updated analysis of RTOG 94–13, with emphasis on unexpected hormone/radiation interactions. Int J Radiat Oncol Biol Phys 2007;69(3):646–55.
[17] Pommier P, Chabaud S, Lagrange JL, Richaud P, Le Prise E, Wagner JP, et al. Is there a role for pelvic irradiation in localized prostate adenocarcinoma? Update of the long-term survival results of the GETUG-01 randomized study. Int J Radiat Oncol Biol Phys 2016;96(4):759–69.
[18] Widesott L, Pierelli A, Fiorino C, Lomax AJ, Amichetti M, Cozzarini C, et al. Helical tomotherapy vs. intensity-modulated proton therapy for whole pelvis irradiation in high-risk prostate cancer patients: dosimetric, normal tissue complication probability, and generalized equivalent uniform dose analysis. Int J Radiat Oncol Biol Phys 2011;80(5):1589–600.
[19] Chuong MD, Hartsell W, Larson G, Tsai H, Laramore GE, Rossi CJ, et al. Minimal toxicity after proton beam therapy for prostate and pelvic nodal irradiation: results from the proton collaborative group REG001-09 trial. Acta Oncol 2017.1-7002E.
[20] Fiorino C, Alongi F, Perna L, Broggi S, Cattaneo GM, Cozzarini C, et al. Dose-volume relationships for acute bowel toxicity in patients treated with pelvic nodal irradiation for prostate cancer. Int J Radiat Oncol Biol Phys 2009;75(1):29–35.

[21] Roeske JC, Bonta D, Mell LK, Lujan AE, Mundt AJ. A dosimetric analysis of acute gastrointestinal toxicity in women receiving intensity-modulated whole-pelvic radiation therapy. Radiother Oncol 2003;69(2):201–7.
[22] Henderson RH, Hoppe BS, Marcus Jr RB, Mendenhall WM, Nichols RC, Li Z, et al. Urinary functional outcomes and toxicity five years after proton therapy for low- and intermediate-risk prostate cancer: results of two prospective trials. Acta Oncol 2013;52(3):463–9.
[23] Fang P, Mick R, Deville C, Both S, Bekelman JE, Christodouleas JP, et al. A case-matched study of toxicity outcomes after proton therapy and intensity-modulated radiation therapy for prostate cancer. Cancer 2015;121 (7):1118–27.
[24] Mondlane G, Gubanski M, Lind PA, Ureba A, Siegbahn A. Comparative study of the calculated risk of radiation-induced cancer after photon- and proton-beam based radiosurgery of liver metastases. Physica Med: PM: Int J Devoted Appl Phys Med Biol: Official J Italian Assoc Biomed Phys (AIFB) 2017.
[25] Park PC, Zhu XR, Lee AK, Sahoo N, Melancon AD, Zhang L, et al. A beam-specific planning target volume (PTV) design for proton therapy to account for setup and range uncertainties. Int J Radiat Oncol Biol Phys 2012;82(2):e329–36.
[26] Lowe M, Albertini F, Aitkenhead A, Lomax AJ, MacKay RI. Incorporating the effect of fractionation in the evaluation of proton plan robustness to setup errors. Phys Med Biol 2016;61(1):413–29.
[27] Pugh TJ, Amos RA, Baptiste SJ, Choi S, Nguyen QN, Zhu XR, et al. Multi-field optimization intensity-modulated proton therapy (MFO-IMPT) for prostate cancer: robustness analysis through simulation of rotational and translational alignment errors. Med Dosimetry: Off J Am Assoc Med Dosimetrists 2013;38 (3):344–50.
[28] Paganetti H. Range uncertainties in proton therapy and the role of Monte Carlo simulations. Phys Med Biol 2012;57(11):R99–R117.
[29] Yang M, Virshup G, Clayton J, Zhu XR, Mohan R, Dong L. Theoretical variance analysis of single- and dual-energy computed tomography methods for calculating proton stopping power ratios of biological tissues. Phys Med Biol 2010;55(5):1343–62.
[30] Bar E, Lalonde A, Royle G, Lu HM, Bouchard H. The potential of dual-energy CT to reduce proton beam range uncertainties. Med Phys 2017;44(6):2332–44.
[31] Soukup M, Sohn M, Yan D, Liang J, Alber M. Study of robustness of IMPT and IMRT for prostate cancer against organ movement. Int J Radiat Oncol Biol Phys 2009;75(3):941–9.
[32] Berger T, Petersen JBB, Lindegaard JC, Fokdal LU, Tanderup K. Impact of bowel gas and body outline variations on total accumulated dose with intensity-modulated proton therapy in locally advanced cervical cancer patients. Acta Oncol 2017;56(11):1472–8.
[33] Liu W, Frank SJ, Li X, Li Y, Zhu RX, Mohan R. PTV-based IMPT optimization incorporating planning risk volumes vs robust optimization. Med Phys 2013;40(2):021709.
[34] Liu W, Zhang X, Li Y, Mohan R. Robust optimization of intensity modulated proton therapy. Med Phys 2012;39(2):1079–91.